Chapter 2

Model system for exciton diffusion characterization

Summary

Exciton diffusion and photoluminescence quenching in conjugated polymer/fullerene heterostructures are studied by time-resolved photoluminescence. It is observed that heterostructures consisting of a spin-coated poly(*p*-phenylene vinylene) (PPV)-based derivative and evaporated C_{60} are ill-defined because of diffusion of C_{60} into the polymer, leading to an overestimation of the exciton diffusion length. This artifact is resolved by the use of a novel, thermally side-chain polymerizing and cross-linking fullerene derivative (F2D) containing two diacetylene moieties, forming a completely immobilized electron acceptor layer. With this heterostructure test system, an exciton diffusion length of 5 ± 1 nm is derived for this PPV derivative from time-integrated luminescence quenching data.

2.1 Introduction

Photovoltaic devices based on conjugated polymers and fullerenes [1,2] are attractive because of their mechanical flexibility and simple and potentially low-cost fabrication [3]. The most efficient solar cells, based on bulk heterojunctions of poly(*p*-phenylene vinylene)s (PPVs) and fullerene derivatives, have a characteristic power-conversion efficiency of 2.5-3% [4, 5] and incident-photon-to-collected-electron efficiency of around 50% [6]. The photoactive layer of these solar cells consists of an interpenetrating network of conjugated polymer and fullerene, with a polymer fraction of no more than 25 wt % [7]. This relatively small fraction is responsible for a main portion of the light absorption since the most widely used [60]fullerene derivatives, like [6,6]-phenyl C_{61} butyric acid methyl ester (PCBM), have a low absorption coefficient in the visible range of the spectrum. The excitons photogenerated in the polymer phase migrate toward the polymer/fullerene interface where electron transfer from the polymer (donor) to the fullerene (acceptor) takes place. In poly[2-methoxy-5-(3′,7′-dimethyl-octyloxy)-*p*-phenylene vinylene] (MDMO-PPV):PCBM blends, this electron transfer occurs within tens of femtoseconds, whereas the back transfer is in the millisecond range [8]. Consequently, the diffusion of excitons toward the polymer/fullerene heterojunction is an important process with regard to the efficiency of the device. The exciton diffusion length determines the size of the polymer phase that is effective in the charge carrier generation process. Enhanced exciton diffusion allows for larger polymer domains, hence for an increase of the fraction of polymer in the blend, which in turn gives rise to an increased absorption (in the case of a weakly absorbing acceptor).

The exciton diffusion lengths in various conjugated polymers reported in the literature show a large variation, ranging from 5 to 14 nm [9–12]. Most of these studies make use of a bilayer model system, comprising an evaporated C_{60} layer in combination with a conjugated polymer, spin-coated from solution. Comparatively, from photocurrent measurements on precursor PPV/C60 photovoltaic devices, an exciton diffusion length of 7 ± 1 nm has been deduced [11]. In this work, it was stressed that a precursor PPV with a relatively high glass transition temperature was used in order to avoid C_{60} interdiffusion into the relatively soft PPV layer. From photocurrent spectra on the same material combination, an exciton diffusion length of 12 ± 3 nm has been derived [12]. A more direct way, which decouples the device performance (photocurrent) from the exciton diffusion, is to study the quenching of the photoluminescence from polymer/fullerene bilayer heterostructures. The photogenerated exciton population is directly probed in this approach. The change of the photoluminescence with varying polymer layer thickness in a heterostructure directly reflects the change in exciton population due to their diffusion and subsequent charge transfer at the interface. The quenching of the photoluminescence (PL) of a ladder-type conjugated polymer, which was spin-coated on top of a [60]fullerene-derived self-assembled monolayer, has been measured, and an exciton diffusion length of 14 nm has been deduced from these measurements [10]. Furthermore, from the PL quenching of heterojunctions consisting of polythiophene and evaporated C_{60}, an exciton diffusion length of 5 nm has been obtained [9].

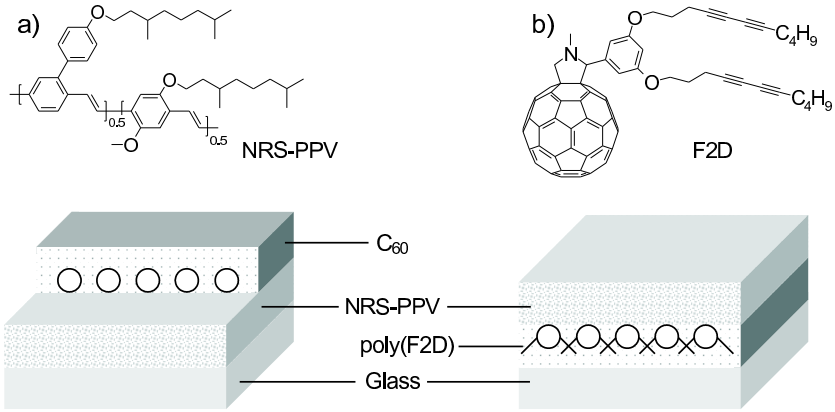

Figure 2.1: Schematic diagram of the sample configuration. C_{60} is evaporated on part of the polymer film (a). The poly(F2D) layer is formed by spin-coating and subsequent thermal polymerization/cross-linking of the F2D monomer layer. Subsequently, the NRS-PPV polymer is spun on top (b).

A disadvantage of the precursor PPVs [11, 12] is that they are not applicable in bulk heterojunction devices. In the present study, we investigate the exciton diffusion length in a random copolymer of poly(2-methoxy-5-(3′,7′-dimethyloctyloxy)-*p*-phenylene vinylene) and poly[4′-(3,7-dimethyloctyloxy)-1,1′-biphenylene-2,5-vinylene] (NRS-PPV, Figure 2.1a), which is a soluble PPV derivative. It is demonstrated that evaporation of C_{60} on top of these spin-coated layers results in ill-defined heterostructures. The C_{60} diffuses into the polymer layer on a time scale of several hours. As a result, analysis of the photoluminescence quenching of such a heterostructure leads to a strong overestimation of the exciton diffusion length. This problem can be circumvented by the use of an immobilized acceptor layer. For this purpose, a new fullerene derivative with two diacetylene moieties is developed (F2D, see Figure 2.1b), which can be polymerized in the solid state. After polymerization, the resulting poly(F2D) layer is completely insoluble, and well-defined heterostructures can be constructed with any soluble material on top of it. Therefore, it serves as an ideal substrate acceptor material to study exciton diffusion in soft materials such as conjugated polymers. Photoluminescence quenching measurements on NRS-PPV/poly(F2D) heterostructures were performed, and an exciton diffusion length of 5 ± 1 nm was obtained. This is in agreement with earlier reported results [11], where C_{60} in-diffusion was prevented as much as possible by choosing a "hard"precursor PPV.

2.2 Experiment

Sample preparation. Synthesis of fullerene derivatives used in this study is described in detail elsewhere [13]. In Figure 2.1, an overview is given of the typical sam-

ple configuration and the materials used in this study. Two types of donor-acceptor bilayer systems were fabricated on top of glass substrates. In the first structure, thin films of NRS-PPV were deposited by spin casting from a toluene solution in nitrogen atmosphere. A series of NRS-PPV layer thicknesses ranging from 4 to 165 nm were obtained by varying the polymer solution concentration and spin frequency. Subsequently, glass/NRS-PPV/C_{60} structures were prepared by evaporation of C_{60} on top of the polymer film under high vacuum ($P < 3 \times 10^{-7}$ mBar) with an evaporation rate of about 0.05 nm/s. In the second structure, the fulleropyrrolidine monomer (F2D, Figure 2.1b) was spin-coated from a chlorobenzene solution on top of the glass substrate to yield a 40 nm thick layer. Full thermopolymerization of the fullerene layer was achieved during 20 minutes at 250 °C to obtain a completely insoluble film of poly(F2D). Subsequently, NRS-PPV in a toluene solution was spin-coated on top. The film thicknesses and surface roughness were characterized by a surface profilometery (Dektak 6M), by optical absorption spectroscopy, and by atomic force microscopy.

Optical techniques. The quenching of the luminescence can be monitored by either measuring the change of the luminescence decay using time-resolved measurements or by measuring the absolute steady-state luminescence output using an integrating sphere. The advantage of the first approach is that it is less sensitive to slight variations in the experimental conditions, since the decay curve can be normalized to its maximum value. Time-resolved optical experiments were carried out with the output of a mode-locked femtosecond Ti:sapphire laser. Laser pulses (pulse width of 150 fs, repetition rate of 4 MHz) were frequency-doubled, and PPV excitation was performed at 400 nm, with p-polarized light at 64∘ incident angle in order to minimize internal reflections. Typical time-averaged excitation intensities on the sample were about 30 mW/cm^2. Exciton-exciton 'bimolecular' quenching interactions are ruled out at this excitation conditions as the exciton densities are well below the threshold for amplified spontaneous emission or exciton-exciton annihilation [14,15]. Emission was collected normal to the excitation beam. To avoid degradation, samples were sealed under nitrogen in a cell with a quartz window. In time-correlated single photon counting (TCSPC) experiments [16], an instrument response function of 30 ps (full width at half-maximum) was used for the deconvolution of the luminescence decay. For consistency, luminescence quenching for the same samples of NRS-PPV polymer layers partly covered with C_{60} was also obtained by steady-state measurements, using an integrating sphere (Labsphere) with argon-ion laser (Spectra-Physics) excitation at 458 nm. The results of the time-resolved data were found to be identical to the results obtained from these steady-state measurements in the test samples used for this comparison. In this study, the time-resolved data are presented to analyze the luminescence quenching and exciton diffusion experiments over the whole range of thicknesses measured. All optical experiments were performed at room temperature.

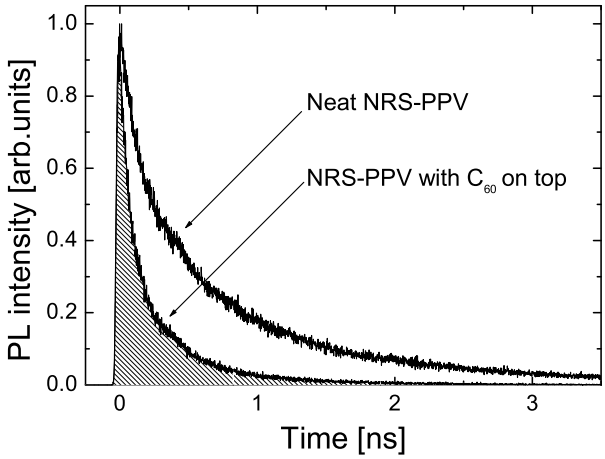

Figure 2.2: Normalized photoluminescence decay of 30 nm NRS-PPV film with and without evaporated C_{60} on top, measured at the emission maximum of 580 nm.

2.3 Time-integrated PL quenching model

In Figure 2.2, we show the normalized photoluminescence decay curves of a 30 nm NRS-PPV film with and without evaporated C_{60} on top, as obtained by TCSPC measurements. The devices were excited from the PPV side at a wavelength of 400 nm, and the emission was collected at 580 nm, which corresponds to the maximum of the luminescence spectrum. The PL of the sample covered with C_{60} obviously decays faster, which is attributed to the luminescence quenching by the efficient electron transfer from the PPV donor to the C_{60} acceptor. This short-range exciton capture occurs with a characteristic time of 45 fs [17] and agrees well with the high internal conversion efficiencies (more than 85%) reported for conjugated polymer/fullerene PV cells [4]. However, in solutions of model oligo(*p*-phenylene vinylene) fulleropyrrolidine dyads (OPVn-C_60) the exciton capture by a fullerene has been shown to occur via an energy transfer from the OPV moiety to the C_60 moiety with a characteristic time constant of 200 fs [18]. A way to disentangle these mechanisms would be to choose an acceptor with an excited state energy level higher than the singlet excited state level of PPV, since this would completely exclude the possibility of an energy transfer mechanism.

To simulate the quenching of the excited states in the polymer layer, the following one-dimensional continuity equation for the photoexcitation density [9, 10] $n(x,t)$ is used

$$\frac{\partial n(x,t)}{\partial t} = -\frac{n(x,t)}{\tau_0} + D\frac{\partial^2 n(x,t)}{\partial x^2} - S(x)n(x,t) + g(x,t). \tag{2.1}$$

The spatial variable x represents the distance from the glass/polymer interface. The first term on the right-hand side of Eq. (2.1) accounts for the process of radiative and

nonradiative decay of the excited states in the neat polymer film, characterized by a single exponential decay time constant τ_0. The second term is the one-dimensional exciton diffusion characterized by the diffusion coefficient D. The dissociation of photoexcitations via electron transfer at the polymer/fullerene interface is represented by the third term. The last term describes the exciton generation process and is governed by the spatially dependent intensity of the femtosecond laser pulse.

The characteristic distance of exciton diffusion in one dimension is the exciton diffusion length, defined as

$$L_D = \sqrt{D\tau_0}. \tag{2.2}$$

For the further model construction, we assume an infinite exciton quenching rate at the polymer/fullerene interface. This implies an exciton diffusion-limited luminescence quenching in polymer/fullerene heterostructures. Two decades ago, it had been extensively demonstrated that a similar model, applied in molecular crystals with exciton traps, can cause a dramatic underestimation of the characteristic diffusion parameters: diffusion constant D and diffusion length L_D [19]. This originates from the fact that two distinct rates govern the total exciton quenching process: the rate at which excitons migrate into the regions occupied by trap molecules, quantified by the diffusion term in Eq. (2.1), and the rate at which an excitation decays to the trap states from neighboring host molecules once it approaches a trap, described by the dissociation (capture) term in Eq. (2.1) given by $-S(x)n(x,t)$. Thus, luminescence quenching by exciton traps introduced into *organic crystals* has been proven to be capture- but not motion-limited, which results from the fact that the exciton motion is faster then the exciton capture by traps. In our study, we consider the slow (activated) exciton diffusion in *highly disordered* conjugated polymers, driven by a hopping mechanism between long chain segments [20]. This slow diffusion occurs after picosecond exciton relaxation within an inhomogeneously broadened density of states (DOS) [21]. The dwell time of an excitation in PPV is estimated to be on the order of ~ 3 ps [22]. In contrast, a short-range exciton capture by the efficient electron transfer from the conjugated polymer to the fullerene [23] occurs with a characteristic time of 45 fs [17]. Therefore, the dwell time between consequent hopping steps in the investigated diffusion process in conjugated polymer is much longer then the exciton quenching time at the polymer/fullerene interface. Unlike in organic crystals, this strongly suggests that the exciton quenching in conjugated polymer/fullerene heterostructures is truly diffusion-limited. As a helpful method to discriminate between capture and motion effects, surface-quenched time-resolved luminescence experiments have been also suggested [19, 24]. Recent time resolved luminescence decay measurements in conjugated polymer/fullerene heterostructures confirmed the dominance of diffusion-limited exciton quenching [25].

Consequently, Eq. (2.1) can be simplified by assuming an infinite exciton quenching rate at the polymer/fullerene interface, without any x dependence. As a result the term responsible for surface quenching can be removed, and for a polymer film with thickness L, the boundary condition $n(x = L) = 0$ at the polymer/fullerene interface is used. At the interfaces with no fullerene present (i.e., the polymer/nitrogen and substrate/polymer interfaces), we use the boundary condition $\partial n/\partial x = 0$ assuming

low surface quenching [9].

The relative quenching efficiency Q, is defined as one minus the number of photons emitted from the polymer film with C_{60} evaporated on top, normalized to the number of emitted photons from the neat polymer film with equal thickness

$$Q(L, L_D) = 1 - \frac{\int_0^\infty \int_0^L n_{\text{pol./fullerene}}(x, t, L_D) dx dt}{\int_0^\infty \int_0^L n_{\text{neat pol.}}(x, t, L_D) dx dt}. \tag{2.3}$$

The integrals in Eq. (2.3) represent the total time-integrated photoluminescence of the polymer films with and without the C_{60} layer, respectively. Consequently, Q is a function of the polymer film thickness L as well as the exciton diffusion length L_D.

To obtain the exciton diffusion length, Eq. (2.3) has to be fitted to the luminescence quenching efficiency data, with the photoexcitation density $n(x, t, L_D)$ governed by Eq. (2.1). The time-integrated approach, used to obtain the quenching efficiency Q, is equivalent to steady-state quenching, and the exciton density distribution time derivative in Eq. (2.1) can be set to zero. Then the exciton quenching efficiency Q as a function of polymer film thickness L is given by

$$Q = \frac{[a^2 L_D^2 + a L_D \tanh(L/L_D)] \exp(-aL) - a^2 L_D^2 [\cosh(L/L_D)]^{-1}}{(1 - a^2 L_D^2)[1 - \exp(-aL)]}, \tag{2.4}$$

with a as the absorption coefficient and L_D the exciton diffusion length as defined above (Eq. (2.2)), being the only fit parameter in this model.

2.4 PL quenching in PPV/C_{60} structures

To quantify the luminescence quenching efficiency from the time-resolved data, the luminescence decay curves for the samples with different polymer thicknesses were normalized, and the areas under the curves were determined, representing the time-integrated emission (Fig. 2.2). Upon reduction of the polymer film thickness, a larger portion of the excited states will reach the polymer/C_{60} interface. As a result, the relative quenching efficiency will increase, as is represented by symbols in Fig. 2.3a.

The best fit (Fig. 2.3a, solid line) is obtained for a diffusion length of 28 nm in the NRS-PPV/C60 sample. This value is several times higher than all other values reported in the literature for conjugated polymers (7-14 nm) [9–12]. A possible explanation for this very long quenching length could be the intermixing of the evaporated C_{60} molecules with the soft polymer layer, which would obscure the intrinsic exciton diffusion process. From photoelectron spectroscopy and X-ray absorption, it has been demonstrated that C_{60} diffuses at room temperature into a spin-coated poly(3-octylthiophene) (P3OT) layer after deposition by evaporation [26]. The time scale of this in-diffusion process of C_{60} into P3OT typically amounts to half an hour. With this in mind, we followed the time dependence of the luminescence quenching efficiency for a NRS-PPV film after evaporation of a C_{60} film (Fig. 2.4). The time required to vent the evaporator, take out the devices, mount them in the optical setup,

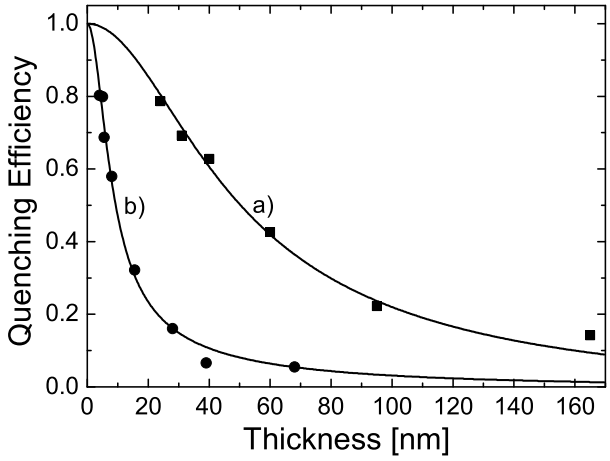

Figure 2.3: The relative luminescence quenching in polymer/C_{60} (a) and polymer/poly(F2D) (b) heterostructures for different polymer film thicknesses. Fits of these data with Eq.(2.3) (solid lines) using exciton diffusion lengths of 28 nm and 5 nm for (a) and (b), respectively, are shown.

and perform the first time-resolved PL scans was typically 20-25 min. After this period, it is clearly observed from Fig. 2.4 that the luminescence quenching yield of the 26 nm NRS-PPV layer is still increasing in time, indicative of a slow C_{60} diffusion into the polymer film. After typically two hours, the quenching length approaches its maximum value of 28 nm as shown in the inset of Fig. 2.4, which gives an indication about the C_{60} diffusion rate at room temperature. From the measured quenching lengths and corresponding time dependence, it is clear that evaporation of C_{60} on top of spin-coated conjugated polymers leads to ill-defined heterojunctions. Therefore, in these devices, it is not possible to obtain information about the intrinsic exciton diffusion process in NRS-PPV.

2.5 Side-chain cross-linked fullerene/PPV heterojunctions

One solution to measure the intrinsic values of exciton diffusion is to choose a polymer with a high glass transition temperature [11] as a precursor PPV, to prevent C_{60} interdiffusion as much as possible. A disadvantage of this approach is that it is not applicable to the soluble polymers that are used in photovoltaic devices, based on blends of PPV and fullerenes. In this study, an alternative approach is presented: instead of an evaporated C_{60} layer as an acceptor, we use a side-chain cross-linked fullerene layer.

Thermal polymerization and cross-linking are preferred for this fullerene layer,

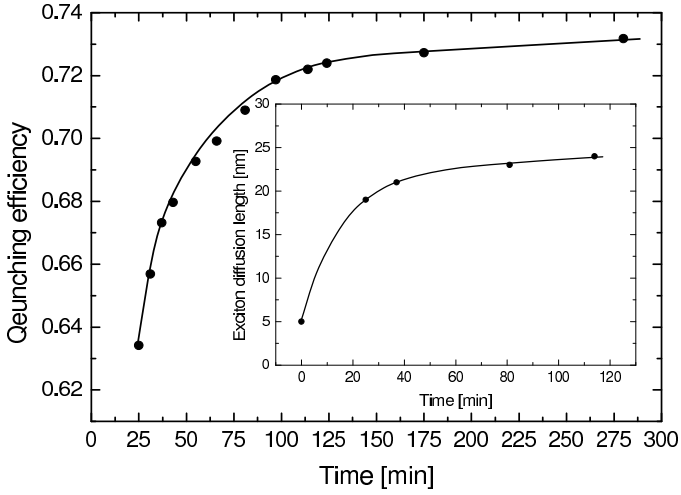

Figure 2.4: Growth of the relative quenching for the 26 nm polymer film with evaporated C_{60} on top in time. The C_{60} evaporation starts at $t = 0$. The inset shows the increase of the apparent exciton diffusion distance as a function of time.

because light-induced polymerization can be complicated due to the absorption of a large portion of the light by the fullerene, thus reducing the desired side-chain reactivity of the monomer and opening pathways for fullerene-related photochemical reactions. A possible thermally polymerizable system is a fullerene derivative containing two or more diacetylene groups. Diacetylenes can be thermally polymerized, and this reaction is rapid [27], which is convenient from a practical point of view. Preferably, the process should take place in the solid state, to prevent, for example, dewetting of the substrates or mixing of the molten fullerene layer with an underlying organic layer, if such a layer is present.

Hirsch and co-workers have already reported a system comparable to that discussed above [28,29]. They demonstrated photochemical polymerization of a so-called hexakis Bingel adduct containing 12 diacetylene groups. However, there are a few drawbacks to the use of their system. A large number of diacetylene-functionalized alkyl chains per fullerene unit were needed to obtain insoluble films [29]. Hexakis adducts of C_{60} are expected to be far less effective as the quenching layer materials (compared to monoadducts) in our photoluminescence quenching experiments. Also, the reaction reportedly took several days, and it occurred in the liquid state. As mentioned above, this is not ideal, and therefore, an improved system was developed, which can be polymerized in the solid state.

The structure and synthesis of the polymerizable fullerene derivative F2D that was used in this study are shown in Figure 2.1b and Figure 2.5, respectively. F2D is a so-called Prato adduct and contains two diacetylene groups, because at least two such groups per fullerene unit are required to obtain both polymerization and three-

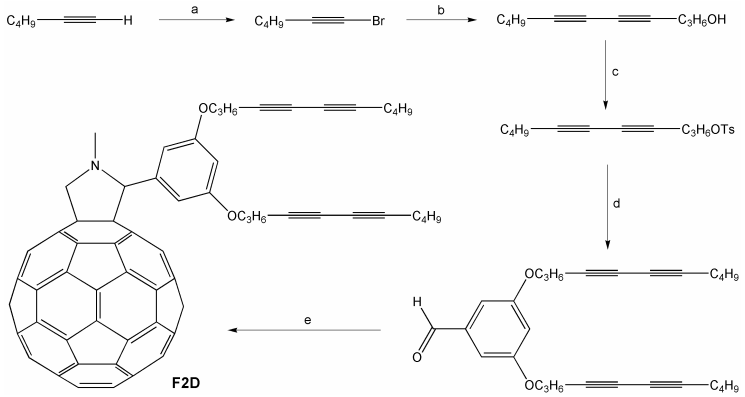

Figure 2.5: Synthesis of F2D. (a) NaOH, Br_2, H_2O/THF, 96 h, 61%. (b) 4-pentyn-1-ol, CuI, C_4H_9N, 3 h, 80%. (c) TsCl, C_5H_5N, 0 °C, 20 h, 75%. (d) 3,5-dihydroxybenzaldehyde (0.5 equiv), K_2CO_3, NaI, DMF, 55 °C, 48 h, 55%. (e) C_{60}, $NH(CH_3)CH_2COOH$, C_6H_5Cl, 85 °C, 20 h, 31%.

dimensional cross-linking. This cross-linking is necessary in order to obtain a really insoluble fullerene film from the processable monomer. The presence of more than two diacetylene groups would in theory be superfluous. Relatively short alkoxy spacers containing only three methylene groups are present between the diacetylene moieties and the aryl group that links them to the fulleropyrrolidine. This structure was chosen, because the reactive groups have a reasonable amount of flexibility, while at the same time, the amount of inactive material (i.e., alkyl groups) is kept at a minimum, which is relevant if such derivatives are to be used for (opto)electronic applications. The butyl end groups approximately match the length of the propyloxy spacers, thus allowing for possible interdigitated structures. Besides, 1-bromo-1-alkynes smaller than 1-bromo-1-hexyne are inconvenient from a synthetic point of view [30].

The appropriate diacetylene-containing alkyl chains were prepared by a selective cross-coupling of 4 pentynol with 1-bromo-1-hexyne, using an excess of the latter. This is in contrast to the original procedure [31], where the best results were obtained using an excess of the acetylenic alcohol. However, in our experiments it was found that in that case the product after chromatography always contained a residual amount of this alcohol, which was difficult to remove completely [32] and would give side products in subsequent steps. Thus, the modified procedure was preferred. The alcohol group was converted into the tosylate, and the resulting compound was then coupled with 3,5-dihydroxybenzaldehyde. Finally, a Prato reaction [33] of this benzaldehyde derivative with C_{60} gave the desired fulleropyrrolidine (F2D).

The structure of compound F2D was confirmed by ^1H and ^{13}C NMR and IR spectroscopy, as well as by mass spectrometry. Interestingly, the ortho C atoms of the aryl group seemed to be missing in the ^{13}C NMR spectrum. However, they showed up as a broad peak with low intensity. This is most likely the result of the severely hindered rotation of the phenyl group due to the presence of the two long alkyl chains

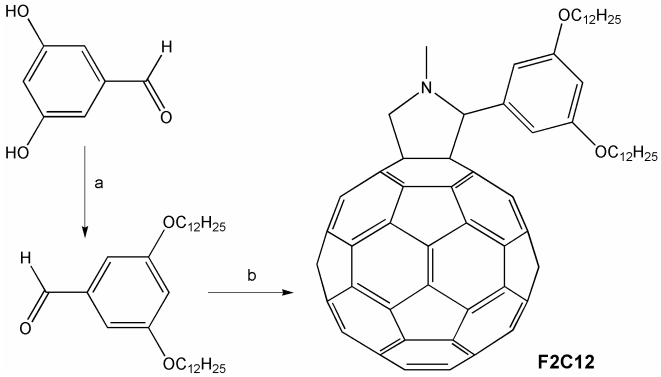

Figure 2.6: Synthesis of F2C12. (a) $C_{12}H_{25}Br$ (2 equiv), K_2CO_3, NaI, DMF, 60 °C, 72 h, 94%. (b) C_{60} (1.5 equiv), $NH(CH_3)CH_2COOH$, C_6H_5Cl, 95 °C, 20 h, 43%.

at the meta positions, which will have to move a long distance through the solvent when the aryl ring rotates [34]. As a result, in addition, the signals from the other aromatic carbons atoms were broadened in the ^{13}C NMR spectrum.

To investigate the thermal polymerization of F2D, films were drop-cast on glass slides and heated in a nitrogen atmosphere on a hotplate at various temperatures for a certain time (usually 0.5, 1, 2, and 3 h). Subsequently, the heated films were tested for their (in)solubility by immersing them in ODCB in a closed test tube for 24 h. These experiments revealed that there was a threshold temperature for polymerization. Below 150 °C, the monomer did not react at all, even after heating for several hours. At around 175 °C, a reaction took place, and films that were virtually insoluble in ODCB were obtained after 2-3 h of heating. At still higher temperatures ($\geq$ 200 °C), the product films became completely insoluble within 30 min of heating. In a series of control experiments, a fulleropyrrolidine bearing two dodecyl groups instead of the two diacetylene-containing alkyl chains (F2C12, see Figure 2.6) showed no reactivity or instability up to at least 250 °C. Heated films of F2C12 always dissolved almost instantly in ODCB after the thermal "annealing"step, and analysis showed only pure monomer. Thus, it was concluded that the formation of the insoluble films must be the result of cross-linking of the diacetylene groups in the film, not of reactions or degradation of the fullerene moiety.

Insoluble films of organic compounds are not easily analyzed in great detail. In this particular case, it is presumed (and desired) that the major part of the molecule (i.e., the fullerene) plays no role in the polymerization process and will remain unchanged. This means that there will be only minor differences in the overall chemical structure of the films before and after, which is a drawback for their analysis. The fullerene derivatives contain mainly sp^2 and sp^3 carbon atoms, which rules out techniques such as XPS, as the disappearance (actually only a decrease) of the small number of sp hybridized carbon atoms will be difficult to detect. UV-vis spectroscopy seems a pos-

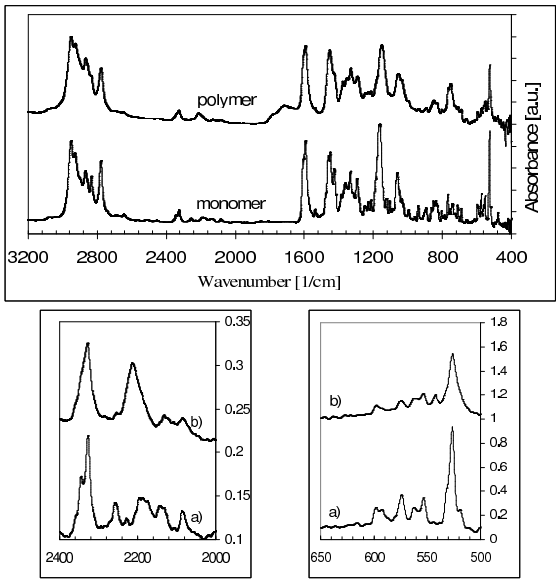

Figure 2.7: IR absorption spectra of F2D (a) and poly(F2D) (b). The insets show enlargements of the two areas that are discussed in the text.

sibility, but for an accurate comparison of the films before and after polymerization, exact repositioning of the substrate after heating is required to eliminate the effects of differences in reflection and/or diffraction of the light. An attempt was made using spin-cast films on quartz slides, but the spectrum after heating showed no new peaks compared to that of untreated F2D. The disappearance of the diacetylene moieties could not be seen, as this absorption is overshadowed by the strong absorptions of the fullerene moiety, and only some broadening in the region of the fullerene absorption was observed. This is most likely because the poly(enyne)s formed in the polymerization/cross-linking will all be of varying length and structure, thus giving rise to a broad, low-intensity absorption.

The reaction of the diacetylene groups was confirmed by IR spectroscopy. After polymerization, the films were scraped from the glass slides using KBr powder for sandpaper, and the resulting dispersions were investigated in diffuse reflection (DRIFT) experiments. In this way, the whole film is analyzed, not just the top layer. The results are shown in Figure 2.7. The two spectra in Figure 2.7 are rather similar. The IR absorptions in the poly(F2D) spectrum have somewhat broadened compared to those of the monomer. All vibrations of those parts of the molecule that are not involved in the polymerization process are still present with their relative intensity virtually unchanged. The only clearly visible change is in the diacetylene vibration at 2258 cm^{-1}, which has disappeared (see inset), and a broad new vibration around 2220 cm^{-1} has appeared. These changes in the spectrum of the material before and after polymerization compare well to those reported in the literature for other poly-

merized diacetylenes [35, 36], indicating that poly(F2D) must have formed and that the reaction has proceeded in the desired manner. The vibrations of the C_{60} moiety seem not to have been affected by the polymerization (see inset). The pattern in the 600-500 cm^{-1} range is highly similar for F2D and poly(F2D). Thus, at least the major part of the fullerenes has not reacted and remains intact. This has been reported before, in a system where diacetylenes were polymerized in the presence of a C_{60} derivative [37].

The poly(F2D) system discussed above is an ideal model system to study exciton diffusion in heterojunctions with any soluble conjugated polymers which are interesting for organic solar cells. After thermal polymerization/cross-linking, the fullerene molecules are immobilized, preventing them from diffusing into the polymer, and the poly(F2D) layer is totally insoluble, even in good fullerene solvents. Since the exciton diffusion length is expected to be on the order of 5-10 nm, it is important to characterize the surface roughness of the poly(F2D) films. F2D spin-cast and thermopolymerized/cross-linked film surface was characterized with atomic force microscopy, and the root-mean-square (RMS) of less than 0.8 nm was determined. Furthermore, we observed that the films are smooth and uniform without interfacial voids, which could mask the intrinsic exciton diffusion length. Consequently, the conjugated polymer can be spin-cast on top of the fullerene layer without any interdiffusion of the two materials taking place.

2.5.1 Exciton diffusion length in NRS-PPV

Glass/poly(F2D)/NRS-PPV samples with varying PPV film thicknesses were prepared by spin-coating NRS-PPV from toluene solution on top of the side-chain polymerized fullerene layer. Luminescence quenching measured on these samples was found to be stable in time, in contrast to the structures with evaporated C_{60} on the polymer, showing the absence of fullerene diffusion into the polymer film. The luminescence quenching observed for this sample structure is relatively small; the results are represented in Fig. 2.3b, circles. By attributing this quenching to the exciton diffusion toward a well-defined polymer/fullerene interface, the experimental data are fitted well by taking an exciton diffusion length of 5 ± 1 nm (Fig.2.3b, solid line). This value is significantly lower than the characteristic quenching range determined from the NRS-PPV/C_{60} heterostructure. The exciton diffusion length of 5 ± 1 nm that we estimated for NRS-PPV is in close agreement with the values found for the precursor PPV (7 ± 1 nm) that was determined by photovoltaic response simulation [11] and for polythiophene as obtained from luminescence quenching (5 nm) [9]. Consequently, in polymer/fullerene photovoltaic devices, the dissociation of excitons is confined to a region of only a few nanometers from the donor/acceptor interface. Our results strongly suggest that the large range of exciton diffusion lengths reported in the literature is due to the interdiffusion of the donor and acceptor materials.

2.6 Conclusions

In conclusion, we have studied photoluminescence quenching in PPV/fullerene heterostructures by means of time-resolved luminescence measurements. It is demonstrated that C_{60} evaporated on top of a spin-coated PPV layer diffuses into the polymer, thereby masking the intrinsic exciton diffusion process. Well-defined PPV/fullerene heterojunctions are obtained by using a newly developed polymerizable fullerene layer made by thermal side-chain polymerization/cross-linking at $\geq$ 200 °C of a fulleropyrrolidine derivative, F2D, that contains two diacetylene moieties. The fullerene layer is cross-linked by polymerization of those diacetylene groups. This has been confirmed by IR spectroscopy and by investigations on a reference compound without the reactive groups (F2C12) that did not react at all. Thus, after thermopolymerization, the acceptor molecules are immobilized, and a sharp heterojunction is obtained between the polymerized fullerene layer and a spin-coated NRS-PPV film. In this model system, an exciton diffusion length of 5 ± 1 nm was obtained.

Bibliography

[1] N. S. Sariciftci, Prog. Quant. Electr. **19**, 131 (1995).

[2] J. J. M. Halls, C. A. Walsh, N. C. Greenham, E. A. Marseglia, R. H. Friend, S. C. Moratti, and A. B. Holmes, Nature (London) **376**, 498 (1995).

[3] C. J. Brabec, N. S. Sariciftci, and J. C. Hummelen, Adv. Funct. Mater. **11**, 15 (2001).

[4] S. E. Shaheen, C. J. Brabec, N. S. Sariciftci, F. Padinger, T. Fromherz, and J. C. Hummelen, Appl. Phys. Lett. **78**, 841 (2001).

[5] M. M. Wienk, J. M. Kroon, W. J. H. Verhees, J. Knol, J. C. Hummelen, P. A. van Hal, and R. A. J. Janssen, Angew. Chem. Int. Ed. **42**, 3371 (2003).

[6] H. Hoppe, N. Arnold, N. S. Sariciftci, and D. Meissner, Sol. Energy Mater. Sol. Cells **80**, 105 (2003).

[7] J. K. J. van Duren, X. Yang, J. Loos, C. W. T. Bulle-Lieuwma, A. B. Sieval, J. C. Hummelen, and R. A. J. Janssen, Adv. Funct. Mater. **14**, 425 (2004).

[8] N. S. Sariciftci and A. J. Heeger, Int. J. Mod. Phys. B **8**, 237 (1994).

[9] M. Theander, A. Yartsev, D. Zigmantas, V. Sundstrom, W. Mammo, M. R. Andersson, and O. Inganas, Phys. Rev. B **61**, 12957 (2000).

[10] A. Haugeneder, M. Neges, C. Kallinger, W. Spirkl, U. Lemmer, J. Feldmann, U. Scherf, E. Harth, A. Gugel, and K. Mullen, Phys. Rev. B **59**, 15346 (1999).

[11] J. J. M. Halls, K. Pichler, R. H. Friend, S. C. Moratti, and A. B. Holmes, Appl. Phys. Lett. **68**, 3120 (1996).

[12] T. Stubinger and W. Brutting, J. Appl. Phys. **90**, 3632 (2001).

[13] D. E. Markov, E. Amsterdam, P. W. M. Blom, A. B. Sieval, and J. C. Hummelen, J. Phys. Chem. A **109**, 5266 (2005).

[14] G. J. Denton, N. Tessler, N. T. Harrison, and R.H.Friend, Phys. Rev. Lett. **78**, 733 (1997).

[15] N. Tessler, G. J. Denton, N. T. Harrison, M. A. Stevens, S. E. Burns, and R. H. Friend, Synth. Met. **91**, 61 (1997).

[16] J. N. Demas, *Excited state lifetime measurements* (Academic Press, New York, 1983).

[17] C. J. Brabec, G. Zerza, G. Cerullo, S. De Silvestri, S. Luzzati, J. C. Hummelen, N. S. Sariciftci, Chem. Phys. Lett. **340**, 232, (2001).

[18] P. A. van Hal, R. A. J. Janssen, G. Lanzani, G. Gurello, M. Zavelani-Rossi, and S. De Silvestri, Phys. Rev. B **64**, 075206 (2001).

[19] V. M. Kenkre, P. E. Parris, and D. Schmid, Phys. Rev. B **32**, 4946 (1985).

[20] L. J. Rothberg, M. Yan, F. Papadimitrakopoulos, M. E. Galvin, E. V. Kwock, and T. M. Miller, Synth. Met. **80**, 41 (1996).

[21] M. Scheidler, U. Lemmer, R. Kersting, S. Karg, W. Riess, B. Cleve, R. F. Mahrt, H. Kurz, H. Bässler, E. O. Gobel, and P. Thomas, Phys. Rev. B **54**, 5536 (1996).

[22] A. Ruseckas, M. Theander, L. Valkunas, M. R. Andersson, 0. Inganäs, and V. Sundström, J. Lumin. **76-77**, 474 (1998).

[23] N. S. Sariciftci, L. Smilowitz, A. J. Heeger, and F. Wudl, Science **258**, 1474 (1992).

[24] P. E. Parris and V. M. Kenkre, Chem. Phys. Lett. **90**, 342, (1982).

[25] D. E. Markov, J. C. Hummelen, P. W. M. Blom, and A. B. Sieval, Phys. Rev. B **72**, 045216 (2005).

[26] C. Schlebusch, B. Kessler, S. Cramm, and W. Eberhardt, Synth. Met. **77**, 151 (1996).

[27] H. -J. Cantow, *Polydiacetylenes* (Berlin: Springer, 1984).

[28] M. Hetzer, H. Clausen-Schaumann, S. Bayerl, T. M. Bayerl, X. Camps, O. Vostrowsky, and A.Hirsch, Angew. Chem. Int. Ed. **38**, 1962 (1999).

[29] F. X. Camps Camprubi, *Thesis* (University of Erlangen, Germany, 1998).

[30] L. Brandsma and H. D. Verkruijsse, Synthesis, 984, (1990).

[31] Based on: M.Alami, ; F.Ferri, Tetrahedron Lett. **37**, 2763, (1996).

[32] The residual 4-pentynol could be removed by prolonged evaporation of volatile materials from the product (several hours in vacuo, using a rotary evaporator). Distillation is not a desirable process for purification of high-boiling diacetylenes, because of their thermal instability.

[33] M. Prato and M. Maggini, Acc. Chem. Res. **31**, 519 (1998).

[34] These same effects were observed for F2C12 and have also been observed in other Prato adducts with comparable structures (P. van 't Hof, R. Valk, and J. C. Hummelen, to be published). There, it was also observed that the effect becomes more severe with increasing length of the alkyl chains. In a few control experiments, ^{13}C NMR measurements were done both in CS_2 and $CDCl_3$, which confirmed that there was no unexpected overlap of the two aromatic CH signals due to the solvent used.

[35] M. del Pilar Carreon, G. Burillo, L. Fomina, and T. Ogawa, Polym. J. **30**, 95 (1998).

[36] M. George and R. G. Weiss, Chem. Mater. **15**, 2879 (2003).

[37] S. -L. Xu, S. -Z. Kang, L. -B. Gan, L. Zhang, C. Wang, L. -J. Wan, and C. -L. Bai, Appl. Phys. A **77**, 757 (2003).